Research and Development Journal
Volume 27 Issue 4 October-December 2016
Received 18 November 2016 Accepted 30 January 2017

PREDICTION OF TIME-DEPENDENT STRENGTHS OF SALT PILLARS USING STRAIN ENERGY PRINCIPLE

The Engineering Institute of Thailand under H.M. The King's Patronage

The Engineering Institute of Thailand under H.M. The King's Patronage

PREDICTION OF TIME-DEPENDENT STRENGTHS OF SALT PILLARS USING STRAIN ENERGY PRINCIPLE

Prapasiri Junthong[1], Prachya Tepnarong[2], Kiattisak Artkhonghan[2] and Kittitep Fuenkajorn[3]
[1]Student, Geomechanics Research Unit, Suranaree University of Technology, Thailand
[2]Lecturer, Geomechanics Research Unit, Suranaree University of Technology, Thailand
[3]Professor, Geomechanics Research Unit, Suranaree University of Technology, Thailand

ABSTRACT

The objective of this study is to determine the long-term strengths of pillars in salt mines in the northeast of Thailand. One of the design requirements is that the pillars must remain mechanically stable up to the time of backfill installation (a minimum of 2-3 years). Strain rate-controlled uniaxial and triaxial compression tests have been performed on salt specimens. The confining pressures are maintained constant ranging from 0, 3, 7 to 12 MPa. The applied strain rates are varied from 10^{-7} to 10^{-4} s^{-1}. The axial stresses and lateral strains are monitored through the strain-softening region for up to 21 days. The results indicate that the strengths and elastic moduli increase exponentially with the applied strain rates. The potential law parameters are calibrated with the test results, and hence allows constructing series of strain-time curves for the pillars subjected to vertical stresses under different depths and extraction ratios. To consider both stress and strain, the strain energy density principle is applied to develop strength criterion for the salt pillars. It is found that the distortional strain energy at dilation and at failure varies linearly with the mean stress (σ_m). Combining this criterion with the series of the strain-time curves the time-dependent strengths of the salt pillars can be predicted.

KEYWORDS: Dilation, Failure, Elastic modulus, Strain Rate, Time-dependency

1. Introduction

Time-dependent deformation of rock salt is commonly determined by subjecting salt specimen to constant deviatoric and mean stresses [1]. The measured strain-time curves can be used to develop constitutive models which can range from simple rheological equations to complex visco-elastic and visco-plastic equations. These models however cannot predict the stress and strain at which the failure occurs. The compressive strength of salt is commonly required for the design of the mine openings. It can be obtained from separated test configurations [2]. Based on the standard practice the salt specimen is subjected to a constant loading rate (normally specified as 0.1 MPa/s). The salt strengths obtained under such relatively rapid loading however may not truly represent those under in-situ condition due to the fact that the mechanical responses of rock salt are sensitive to loading and strain rates [3-5]. To obtain a long-term strength a wider range of loading or strain rates is required to impose on the salt specimens while monitoring the changes of the stresses and strains. The time-dependent strengths are important for the stability analysis of the salt mines and storage caverns. To ensure the long-term stability of the underground structures (e.g., supported pillars, shaft foundations and borehole stability) the relationship between the strength, time and applied stress is needed.

The objective of this study is to determine the time-dependent strengths of rock salt as applied to the stability prediction of salt pillars. The effort involves performing uniaxial and triaxial compression tests under constant axial strain rates ranging from 10^{-7} to 10^{-4} s^{-1}, development of strain energy density criterion at dilation and at failure, and prediction of the time-dependent strength of the salt pillars.

2. Sample Preparation and Test Procedure

Salt core specimens are prepared from salt block collected from an underground salt mine in the northeast of Thailand. They belong to the Lower member of the Maha Sarakham formation. Warren [6] gives the origin and geological description of the formation. The specimens used for the uniaxial and triaxial compression tests are prepared as cylindrical specimens with nominal diameters of 54 mm and lengths of 108 mm. The specimen axis is normal to the bedding planes. The average density is 2.19 ± 0.09 g/cm^3.

The uniaxial and triaxial compression test procedure and calculation are similar to the ASTM standard practice [2]. The constant confining pressures are applied by Hoek cell and are varied from 0, 3, 7 to 12 MPa. The applied constant axial strain rates vary from 10^{-7} to 10^{-4} s^{-1}. The axial strains are controlled using digital displacement transducers and electric pump connected to 100-ton load cell. The loading is applied until the measured axial stress reaches the strain softening region and approaches the defined confining pressure. The axial stress and lateral and volumetric strains are monitored. The modes of failure are identified. A total of 16 specimens have been tested.

3. Test Results

Figure 1 shows the axial stresses (σ_1) as a function of axial (ε_1), lateral (ε_3) and volumetric (ε_v) strains. The specimens loaded under high strain rates show higher peak stress than those under lower strain rates. This is true for all confining pressures. The greater confining pressures yield the higher peak axial stresses and the higher strains at failure. All specimens show strain-softening behavior. The effects of the strain rate on the salt strength become larger under higher confining pressures. Higher strain rates applied result in higher shear strengths and lower shear strains at failure.

Post-test specimens show combination of tensile splitting and compressive shear failures. Table 1 gives the dilation and failure strengths for all specimens. The dilation strength is determined as the point where the specimen volume starts increasing. The elastic moduli (E_t) and Poisson's ratios (ν_t) are determined from the three-dimensional stress-strain relations below dilation strength where the specimen is within elastic range. Assuming that the specimens are isotropic, the shear (rigidity) modulus (G_t) and Lame′ constant (λ_t), and Poisson's ratio (ν_t) and elastic modulus (E_t) can be calculated from the following relations [7]:

$$G_t = (1/2)\cdot(\hat{o}_{oct}/\tilde{a}_{oct}) \tag{1}$$

$$3\sigma_m = (3\lambda_t + 2G_t)\cdot\varepsilon_v \tag{2}$$

$$\nu_t = \lambda_t/(2(\lambda_t + G_t)) \tag{3}$$

$$E_t = 2G_t\cdot(1+\nu_t) \tag{4}$$

where σ_m and ε_v are the mean stress, and volumetric strain at dilation (the point where the elastic parameters are determined). The subscript "*t*" for the elastic parameters is inserted because they are dependent of time, which are different from those obtained from standard testing (e.g. ASTM D7012-07 [2]). Table 1 gives the results of the calculation. The elastic moduli and Poisson's ratios are plotted as a function of strain rate in Figure 2. The time-dependent elastic modulus as observed here agree with those obtained by Fuenkajorn et al. [5]. The decrease of the Poisson's ratio with increasing axial strain rate can be represented by a linear equation, as shown in Figure 2. Good correlations between the equations above with the test data are obtained.

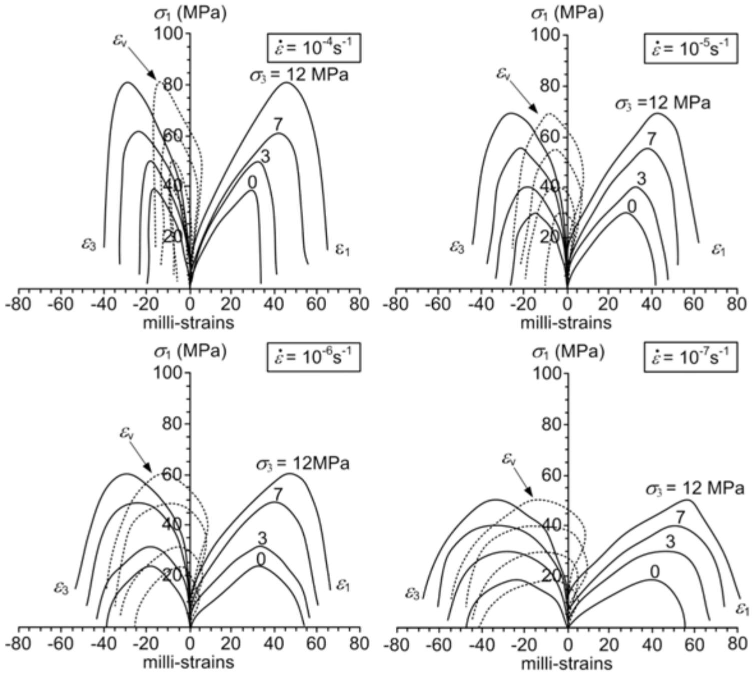

Figure 1 Axial stress (σ_1) as a function of axial (ε_1), lateral (ε_3) and volumetric (ε_v) strains for various confining pressures (σ_3) and strain rates ($\dot{\varepsilon}$)

Table 1 Dilation and failure strengths and elastic parameters

$\dot{\varepsilon}$ (s^{-1})	σ_3 (MPa)	$\sigma_{1,d}$ (MPa)	$\sigma_{1,f}$ (MPa)	G_t (GPa)	λ_t (GPa)	E_t (GPa)	ν_t
10^{-4}	0	25.78	38.67	0.72	2.41	2.51	0.32
	3	31.35	49.12	0.77	3.73	2.59	0.33
	7	40.96	62.92	0.77	2.43	2.99	0.33
	12	53.10	80.59	0.75	2.74	3.82	0.34
10^{-5}	0	20.08	30.03	0.42	1.88	1.31	0.39
	3	27.14	40.10	0.47	2.00	1.42	0.37
	7	39.93	55.38	2.59	0.88	2.07	0.39
	12	51.41	69.88	0.54	2.71	2.34	0.39
10^{-6}	0	14.26	23.68	0.27	1.04	1.02	0.38
	3	25.23	33.26	0.37	1.83	1.10	0.38
	7	37.23	48.29	0.42	2.10	1.65	0.39
	12	45.94	61.65	0.43	2.48	1.92	0.34
10^{-7}	0	12.07	18.64	0.20	0.60	0.55	0.39
	3	21.84	30.97	0.28	1.11	0.79	0.41
	7	30.19	40.89	0.32	1.41	0.99	0.42
	12	39.84	50.13	0.32	1.86	1.10	0.35

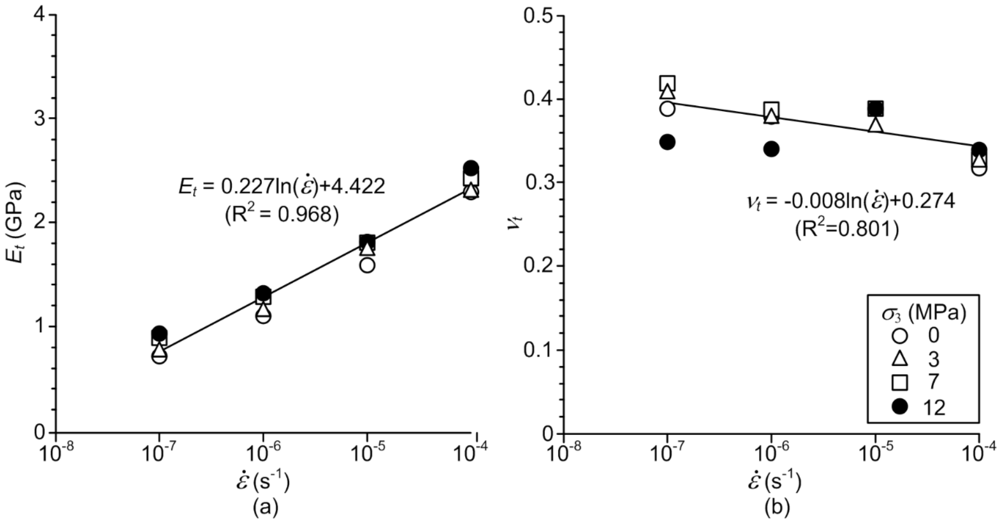

Figure 2 Elastic modulus (a) and Poisson's ratio (b) as function of strain rate $(\dot{\varepsilon})$

4. Strain Energy Density Criterion

In order to incorporate the time-dependent effect into the strength criterion. The strain energy density principle is applied to describe the salt strength and deformability under different strain rates. The distortional strain energy at dilation and failure can be calculated from the octahedral shear stress-strain curves for each triaxial specimen using the following relations:

$$W_d = (3/2)\cdot \int_0^{\gamma_{oct}} \tau_{oct} \cdot d\gamma_{oct} \tag{5}$$

where $\tau_{oct} = \left(\sqrt{2}/3\right)\cdot(\sigma_1 - \sigma_3)$

$\gamma_{oct} = \left(\sqrt{2}/3\right)\cdot(\varepsilon_1 - \varepsilon_3)$

The calculated $W_d - \sigma_m$ relations at dilation and at failure can be represented by a linear relation, as shown in Figure 3. The $W_d - \sigma_m$ relation above can be used as a strength criterion, where it implicitly considers the time-dependent strength of the salt. It is therefore more suitable to describe the salt pillar stability, as compared to the conventional strength criteria that exclude the time-dependent effect.

5. Parameters Calibration

The total strain in salt can be divided into two parts, elastic strain (linear and recoverable strain) and plastic creep strain (time-dependent and norecoverable strain):

$$[\varepsilon^T] = [\varepsilon^e] + [\varepsilon^c] \tag{6}$$

where $[\varepsilon^T]$, $[\varepsilon^e]$ and $[\varepsilon^c]$ are three-dimensional vectors of total, elastic and time-dependent strains.

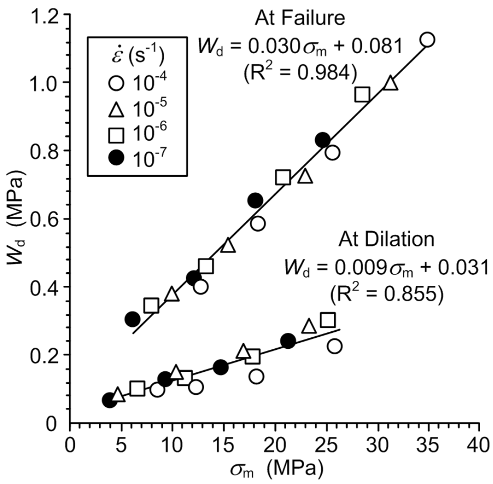

Figure 3 Distortional strain energy (W_d) at dilation and at failure as a function mean stress (σ_m)

The elastic strain for triaxial compression stress state can be obtained from the generalized Hooke's law the axial (principal) strain can be written as:

$$\varepsilon^{e} = (\sigma_1 - 2\nu\sigma_3)/E \quad (7)$$

where ε^e is axial strain, σ_1 is axial stress, σ_3 is confining pressure, E is elastic modulus and ν is Poisson's ratio. These elastic parameters can be obtained from relatively quick loading as those performed by Luangthip et al. [8]. They define these parameters as E = 20.23 GPa and ν = 0.29.

The plastic creep strain can be derived from the theory of plasticity based on the associated flow rule [9-10]. The equivalent creep strain (ε^{*c}) is first obtained from one dimensional creep law which presents the plastic strain as a function of stress and time [11]:

$$\varepsilon^{*c} = \varepsilon^{e} + \kappa\gamma(\frac{2}{3}\cdot\sigma^{*})^{\beta}\cdot t^{\gamma-1} \quad (8)$$

where κ, β and γ are material parameters and σ^* is equivalent (effective) stress.

Based on the von Mises flow rule, σ^* and ε^{*c} are defined as:

$$\sigma^{*} = (1/2)\cdot\left[(\sigma_1-\sigma_2)^2 + (\sigma_2-\sigma_3)^2 + (\sigma_3-\sigma_1)^2\right]^{1/2} \quad (9)$$

$$\varepsilon^{*c} = (1/2)\cdot\left[(\varepsilon_1-\varepsilon_2)^2 + (\varepsilon_2-\varepsilon_3)^2 + (\varepsilon_3-\varepsilon_1)^2\right]^{1/2} \quad (10)$$

Substituting equations (9) and (10) into (8) and taking under triaxial stress (σ_2=σ_3 and ε_2=ε_3) we obtain the following:

$$\frac{\sqrt{2}}{3}(\varepsilon_1-\varepsilon_3) = [(\sigma_1/\mathrm{E}) - (2\nu\sigma_3/\mathrm{E})] + \kappa\gamma\left[\left(\frac{\sqrt{2}}{3}\right)\cdot(\sigma_1-\sigma_3)\right]^{\beta}\cdot \mathrm{t}^{\gamma-1} \quad (11)$$

where ε_1 is axial strain, ε_2 is lateral strain, E = 20.23 GPa and ν = 0.29.

Regression analyses on the equation (11) using test data (σ_1, ι_3, ε_1 and ε_3) with the SPSS statistical software [12] can determine the parameters κ, β and γ for each specimen. Table 2 summarizes the potential law parameters for all confining pressures and axial strain rates. The parameters κ, β and γ tend to be independent of the axial strain rate and confining pressure.

6. Prediction of Time-Dependent Strength of Pillars

The tributary area concept is applied here to determine the pillar stress (σ_p) for the extraction ratios between 30% and 50%. The pillar stress in terms of the extraction ratio (e) can be written as [13]:

Table 2 Potential law parameters based on E = 20.23 GPa and ν = 0.29

Parameters	σ_3 (MPa)	$\dot{\varepsilon}$ (s^{-1})				MEAN ± SD
		10^{-4}	10^{-5}	10^{-6}	10^{-7}	
κ ($\times 10^{-7}$/MPa·s)	0	1.602	1.330	1.209	1.342	1.414 ± 0.19
	3	1.513	1.331	1.599	1.645	
	7	1.257	1.263	1.193	1.519	
	12	1.305	1.272	1.377	1.873	
β	0	2.211	2.310	2.094	2.391	2.219 ± 0.14
	3	2.198	1.986	1.947	2.477	
	7	2.289	2.328	2.221	2.333	
	12	2.234	2.067	2.208	2.206	
γ	0	0.345	0.243	0.243	0.325	0.303 ± 0.06
	3	0.424	0.235	0.324	0.377	
	7	0.357	0.324	0.264	0.233	
	12	0.284	0.244	0.274	0.354	

$$\sigma_P = [(\rho \cdot H)/(1-e)] \times 100 \tag{12}$$

where H is the mine depth, and ρ is in-situ stress gradient of overburden (approx imated here as 0.027 MPa/m). The calculations are made for the depths from 100 to 400 m. The distortional strain energy in salt pillars can be calculated for each depth and extraction ratio, using equation (5).

In order to describe the increase of the pillar deformation (strain) with time under the uniaxial (σ_2=σ_3=0) condition, the potential law in equation (11) can be used. By substituting the material parameters E, ν, κ, β and γ in to equation (11) a series of axial strain-time curves for salt pillars under various depths and extraction ratios can be developed. The pillar strains and their corresponding time at the point where the dilation and failure would occur can be determined by comparing the stresses and time-dependent strains at various pillar ages with the distortional strain energy criterion in Figure 3. Figure 4 shows the time at which the salt pillars reach their dilation and failure points. The results suggest that the duration under stable condition decreases with increasing pillar stresses (or extraction ratios and mine depth). The diagrams can be used as a guideline to ensure that the salt pillars will remain stable up to the time at which the backfill is installed.

7. Discussions and Conclusions

The strain-rate controlled uniaxial and triaxial tests are performed on salt cores under confining pressures of 0, 3, 7 and 12 MPa. The strain-softening behavior can be obtained as suggested by the stress-strain curves. Higher strain rates result in higher peak (failure) strengths. Beyond the dilation point the micro-cracks are probably induced which lead to an increase of the salt specimen volume (Figure 1). The specimen laterally dilated beyond the original volume after the peak strength has been reached. A higher strain rate applied results in a higher elastic modulus of the salt

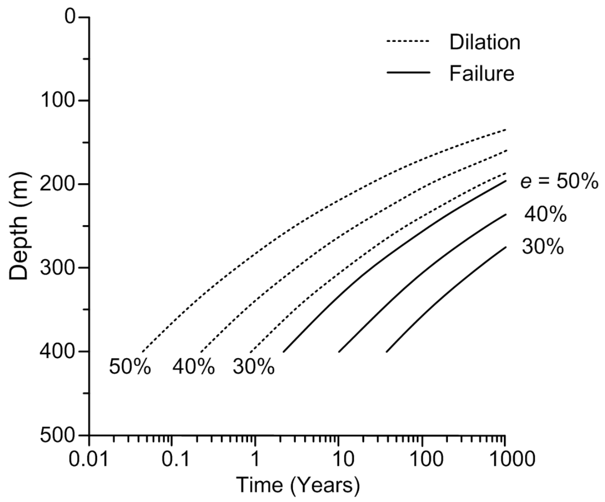

Figure 4 Design criteria representing mining depths as a function of time at dilation and at failure

(Figure 2). The Poisson's ratios decrease with increasing strain rates. The distortional strain energy required to dilate and to fail the specimens can be calculated and presented as a function of the mean stress.

By calibrating the potential law against the test results, the pillar vertical strain under any vertical stress can be described as a function of time. The pillar distortional strain energy at dilation and at failure can therefore be determined and used to calculate the corresponding strains and time after excavation. The strength criterion based on the strain energy principle is probably more suitable and conservative than the conventional strength criteria. This is because it can incorporate the time-dependent effect by considering both salt strengths and strain at dilation and at failure under various deformation rates. This also suggests that obtaining the salt strengths under a wider range of the strain rates would enhance the representativeness of the proposed strain energy criterion.

The simplified approach of pillar design presented here is merely to demonstrate the potential application of the strain energy criterion for the analysis of salt structures. It is based on the tributary area concept while ignoring the shape (height-to-width ratio) size, and end effects. A more comprehensive analysis on these and other relevant factors would be needed to obtain a more realistic design result, which depends upon the site-specific conditions and engineering requirements.

Acknowledgements

This study is funded by Suranaree University of Technology and by the Higher Education Promotion and National Research University of Thailand. Permission to publish this paper is gratefully acknowledged.

References

[1] American Society for Testing and Materials. Standard test methods for creep of rock core under constant stress and temperature (ASTM D7070-08), Annual Book of ASTM Standards, West Conshohocken, 2008.

[2] American Society for Testing and Materials. Compressive Strength and Elastic Moduli of Intact Rock Core Specimens under Varying States of Stress and Temperatures (ASTM D7012-07), Annual Book of ASTM Standards, West Conshohocken, 2007.

[3] Liang, W. G., Zhao, Y. S., Xu, S. G., & Dusseault, M. B. (2010). Effect of strain rate on the mechanical properties of salt rock. *International Journal of Rock Mechanics & Mining Sciences* 48, 161-167.

[4] Fuenkajorn, K. & Daemen, J. J. K. *Borehole closure in salt*. Technical Report Prepared for the U.S. Nuclear Regulatory Commission, Washington DC, 1988, Report No. NUREG/CR-5243 RW.

[5] Fuenkajorn, K., Sriapai, T., & Samsri, P. (2012). Effects of loading rate on strength and deformability of Maha Sarakham salt. *Engineering Geology* 135-136, 10-23.

[6] Warren, J. Evaporites: Their Evolution and Economics, Blackwell Science, Oxford, 1999.

[7] Jaeger, J. C., Cook, N. G. W., & Zimmerman, R. W. (ed.) Fundamentals of Rock Mechanics, 4th edn. Blackwell, Oxford, 2007.

[8] Luangthip, A., Khamrat, S. & Fuenkajorn, K. Effects of carnallite contents on stability and extraction ratio of potash Mine, 9th Asian Rock Mechanics Symposium, Bali, Indonesia, 18 - 20 October 2016.

[9] Senseny, P. E. Review of constitutive laws used to describe the creep of salt, Battelle Memorial Institute, Columbus, 1983.

[10] Nair, R.S., Chang, C-Y, Singh, R. D., & Abdullah, A. M. Time-dependent analysis to predict closure in salt cavities. Proceedings of the 4th Symposium on Salt, Cleveland, Ohio, 1974, pp. 129-139.

[11] Nair, K. & Boresi, A. Stress analysis for time-dependent problems in rock mechanics. Proceedings of the 2nd Congress of the International Society for Rock Mechanics, Belgrade, 1970, pp. 531-536.

[12] Wendai, L. Regression analysis, linear regression and probit regression In 13 chapters, SPSS for Windows: statistical analysis, Publishing House of Electronics Industry, Beijing, 2000.

[13] Hoek, E. & Brown, E. T. (1980). Empirical strength criterion for rock masses. *Journal of Geotechnical Engineering Div ASCE* 160(GT9), 1013-1035.